

Structural and Magnetic Characterization of a Tetranuclear Copper(II) Cubane Stabilized by Intramolecular Metal Cation– π Interactions

Raffaello Papadakis,[†] Eric Rivière,[‡] Michel Giorgi,[§] H el ene Jamet,[ ] Pierre Rousselot-Pailley,[†] Marius R eglier,[†] A. Jalila Simaan,^{*,†} and Thierry Tron[†]

[†]Aix Marseille Universit e, CNRS, ISM2 UMR 7313, 13397 Marseille, France

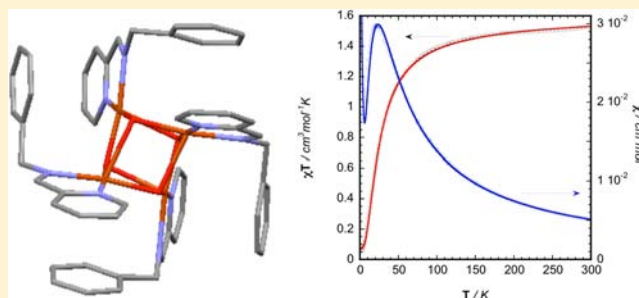
[‡]Universit e Paris-Sud, CNRS, ICMO UMR 8182, 91405 Orsay, France

[§]Aix Marseille Universit e, CNRS, Spectropole FR1739, 13397 Marseille, France

[ ]Universit e Joseph Fourier—Grenoble 1, CNRS, DCM UMR 5250, 38041 Grenoble, France

S Supporting Information

ABSTRACT: A novel tetranuclear copper(II) complex (**1**) was synthesized from the self-assembly of copper(II) perchlorate and the ligand *N*-benzyl-1-(2-pyridyl)methanimine (L^1). Single-crystal X-ray diffraction studies revealed that complex **1** consists of a $Cu_4(OH)_4$ cubane core, where the four copper(II) centers are linked by μ_3 -hydroxo bridges. Each copper(II) ion is in a distorted square-pyramidal geometry. X-ray analysis also evidenced an unusual metal cation– π interaction between the copper ions and phenyl substituents of the ligand. Calculations based on the density functional theory method were used to quantify the strength of this metal– π interaction, which appears as an important stabilizing parameter of the cubane core, possibly acting as a driving parameter in the self-aggregation process. In contrast, using the ligand *N*-phenethyl-1-(2-pyridyl)methanimine (L^2), which only differs from L^1 by one methylene group, the same synthetic procedure led to a binuclear bis(μ -hydroxo)copper(II) complex (**2**) displaying intermolecular π – π interactions or, by a slight variation of the experimental conditions, to a mononuclear complex (**3**). These complexes were studied by X-ray diffraction techniques. The magnetic properties of complexes **1** and **2** are reported and discussed.

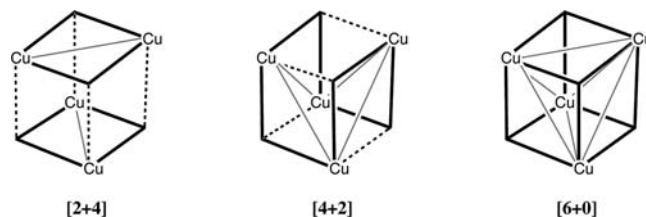


INTRODUCTION

High-nuclearity transition-metal complexes have attracted continuous attention in the past years for their relevance in the fields of both molecular magnetism^{1–3} and bioinorganic chemistry as mimics for multimetal active sites of metalloproteins.⁴ Among polynuclear metal complexes, oxygen-bridged tetrameric copper clusters having a cubane-like Cu_4O_4 core exhibit fascinating plasticity because small structural changes can lead to significantly different magnetic properties.^{5–7}

Mergehenn and Haase have proposed a classification of cubane-like complexes regarding the distribution of long Cu–O distances in the cube.^{8–10} Thus, compounds displaying four long Cu–O distances between two pseudodimeric units have been classified as type I (displaying dominant antiferromagnetic interactions), while compounds with a pair of long distances within each of the pseudodimeric units have been classified as type II (displaying dominant ferromagnetic interactions). A transitional type can also be characterized by intermediate structure and magnetic properties between these extreme structures. Ruiz and collaborators have proposed an alternative classification based on the Cu...Cu distances.¹¹ The cubanes have been divided into three classes (Scheme 1): (i) complexes with

Scheme 1. Schematic Drawing of the Three Types of Cubane Complexes Following the Ruiz et al. Classification^{11a}



^aBold and dotted lines represent the short and long Cu–O distances, respectively. Gray lines show the short Cu–Cu distances.

two short and four long Cu...Cu distances designated as [2 + 4]; (ii) complexes with four short and two long Cu...Cu distances designated as [4 + 2]; (iii) complexes with six equivalent Cu...Cu distances designated as [6 + 0].

Correlations between the structural parameters and magnetic properties for oxygen-bridged copper binuclear complexes or pseudodimeric copper cubanes (type I or [2 + 4]) are well

Received: December 14, 2012

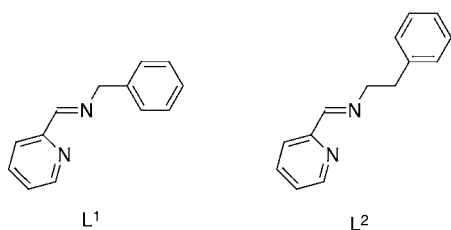
Published: May 3, 2013

established,^{5,6,9,12} while correlations are less simple to establish for other types of cubanes.⁷

Most of the reported cubane structures rely on alkoxy-bridged copper(II) ions when only a limited number of hydroxo-bridged copper(II) complexes have been obtained probably because of increased flexibility of the core.^{13,14} Indeed, only about 15 structures of hydroxo-bridged copper cubanes have been found in the Cambridge Structural Data Base for over more than 100 alkoxy-bridged ones. One challenging issue in the synthesis of metal clusters lies in the understanding and control of the aggregation reactions. To this respect, the design of the ligand as well as the understanding of the structural elements that drive the nuclearity and core geometry of such clusters is of great importance.

Here we report on the synthesis and magnetic characterization of a cubane core hydroxo-bridged copper(II) complex obtained with the ligand *N*-benzyl-1-(2-pyridyl)methaneimine¹⁵ (L^1), as presented in Scheme 2. The copper(II) ions are found to interact

Scheme 2. Ligands Used in This Study



in an unusual cation– π interaction with the benzyl substituents of the ligand. In contrast, using the ligand *N*-phenethyl-1-(2-pyridyl)methaneimine¹⁶ (L^2), which only differs from L^1 by one methylene group, the same synthetic procedure led to a binuclear bis(μ -hydroxo)copper(II) complex displaying intermolecular π – π interactions. Alternatively, a mononuclear complex was obtained with L^2 by slightly varying the experimental conditions. Density functional theory (DFT) calculations were carried out to quantify stabilization of the cubane core provided by metal cation– π interactions. Our results highlight the importance of intra- or intermolecular π -type interactions on the self-aggregation processes.

EXPERIMENTAL SECTION

Syntheses. All solvents and chemicals were purchased from Sigma-Aldrich and used without further purification. **Caution!** Perchlorate salts are potentially explosive and should be handled with care. Syntheses of L^1 and L^2 were performed according to already described procedures.^{15,16}

Synthesis of $[(L^1)_4Cu_4(OH)_4(ClO_4)_4 \cdot H_2O]$ (1). The ligand L^1 (4.70 mmol, 0.922 g) was dissolved in 5 mL of ethanol and then added dropwise to 1 equiv of $Cu(ClO_4)_2 \cdot 6H_2O$ (4.70 mmol, 1.740 g) dissolved in 12 mL of 96% ethanol under reflux. The flask was then immersed in liquid nitrogen in order to induce crystallization. After several days at room temperature, green crystals suitable for crystallographic analysis formed in 35% yield. Selected data for complex 1: FT-IR ν/cm^{-1} 3545 (O–H), 1648 (C=N imine), 1605 and 1451 (pyridine ring), 775 and 746 (C–Hpy), 1027 and 620 (ClO_4^-). Elem anal. Calcd for $C_{52}H_{54}Cl_4Cu_4N_8O_{21}$: C, 40.99; H, 3.57; N, 7.36. Found: C, 41.26; H, 3.33; N, 7.59.

Synthesis of $[(L^2)_2Cu_2(OH)_2(H_2O)_2](ClO_4)_2$ (2). The synthetic procedure is exactly the same as that for complex 1. Blue crystals suitable for crystallographic analysis were obtained. Selected data for complex 2: the crystals were obtained in 45% yield; FT-IR ν/cm^{-1} 3585 (O–H), 1649 (C=N imine), 1604 and 1448 (pyridine ring), 1080 and 621 (ClO_4^-). Elem anal. Calcd for $C_{28}H_{34}Cl_2Cu_2N_4O_{12}$: C, 41.18; H, 4.20; N, 6.86. Found: C, 41.60; H, 4.01; N, 6.82.

Synthesis of $[(L^2)_2Cu(OH)_2](ClO_4)_2$ (3). The ligand L^2 (4.70 mmol, 0.986 g) was dissolved in 96% ethanol. Under reflux, an ethanolic solution containing an equimolar quantity (or alternatively a half-equimolar quantity, as previously described¹⁶) of copper(II) perchlorate hexahydrate was added dropwise. After a couple of days, blue crystals suitable for crystallographic analysis were formed. Yield: 55%. ESI-MS isotopic pattern centered at m/z 241.5799 corresponding to the ion $C_{28}H_{28}N_4Cu^{2+}$: FT-IR ν/cm^{-1} 1640 (C=N imine), 1601 (pyridine ring), 1161, 1102, 1033, and 620 (ClO_4^-). Elem anal. Calcd for $C_{28}H_{30}Cl_2CuN_4O_9$: C, 47.97; H, 4.31; N, 7.99. Found: C, 48.26; H, 4.31; N, 8.02.

Physical Methods. FT-IR spectra were recorded in FT-IR in attenuated total reflection (ATR) mode on a Bruker TENSOR 27 spectrometer equipped with a single-reflection DuraSAMPLIR diamond ATR accessory. ESI-MS analyses were performed using a SYNAPT G2 HDMS (Waters) spectrometer equipped with a pneumatically assisted Atmospheric Pressure Ionization source. The ion-spray voltage was 2.8 kV, the orifice lens was 5 V, and the nitrogen flux (nebulization) was 1200 L h⁻¹. The HR mass spectrum was obtained with a time-of-flight analyzer. A sample was placed in a methanol/3 mM ammonium acetate solution. Elemental analyses were performed using a Thermo Finnigan EA 1112 instrument. The results were validated by at least two measurements.

Crystallographic Measurements. The crystals were mounted on a glass fiber, and data were collected on a Bruker-Nonius Kappa CCD diffractometer at 293 K using Mo $K\alpha$ radiation ($\lambda = 0.71073 \text{ \AA}$). Data collections were performed with COLLECT and cell refinements and data reductions with DENZO/SCALEPACK.¹⁷ The structures were solved with SIR92, and SHELXL-97 was used for full matrix least-squares refinements.^{18,19} The hydrogen atoms on the carbon atoms for all compounds were introduced at geometrical positions and constrained to their parent atom. The hydrogen atoms on the oxygen atoms of the water molecules and the hydroxo bridges were found experimentally and constrained to their parent atom during the refinements. Complex 1 cocrystallized with a water molecule disordered over three sites, the occupancy factors of which were refined to 40%, 30%, and 30%, respectively.

See the Supporting Information for X-ray crystallographic data. The atomic coordinates for these structures have also been deposited with the Cambridge Crystallographic Data Centre. The coordinates can be obtained, upon request, from the Director, Cambridge Crystallographic Data Centre, 12 Union Road, Cambridge CB2 1EZ, U.K.: complex 1, CCDC 915281; complex 2, CCDC 915280; complex 3, CCDC 915279.

Magnetic Measurements. Measurements were performed using a SQUID Quantum Design MPMS 5 magnetometer with an applied field of 1000 Oe. The sample was placed in a gelatin capsule. The susceptibility data were corrected from the contribution of the sample holder and from the diamagnetic contributions, as deduced by using Pascal's constant tables. The errors in the fits (R_χ and $R_{\chi T}$) were calculated from the following expressions, where χ_{obs} and χ_{calc} are the observed and calculated magnetic susceptibilities, respectively:

$$R_\chi = \frac{\sum (\chi_{calc} - \chi_{obs})^2}{\sum \chi_{obs}^2} \quad \text{and}$$

$$R_{\chi T} = \frac{\sum (\chi_{calc} T - \chi_{obs} T)^2}{\sum (\chi_{obs} T)^2}$$

Computational Methods. Theoretical calculations were performed with *wB97XD*,²⁰ a DFT method implemented in the *Gaussian 09* package.²¹ All atoms were described by the triple Ahlrichs TZV basis set.²² Single-point calculation was done using the geometry of the RX structure of complex 1. For the open-shell Cu^{2+} ligand system, calculations were based on an unrestricted formalism. Finally, the counterpoise procedure was used to correct the interaction energy for the basis set superposition error.²³

RESULTS AND DISCUSSION

Synthesis and Structural Characterization. The cubane complex 1 was prepared by addition of the ligand to a solution of copper(II) perchlorate in a 1:1 ratio in 96% ethanol. Green crystals were obtained, and the crystal structure was determined

by single-crystal X-ray diffraction. The molecular structure of the tetranuclear cation of complex **1** is presented in Figure 1, and

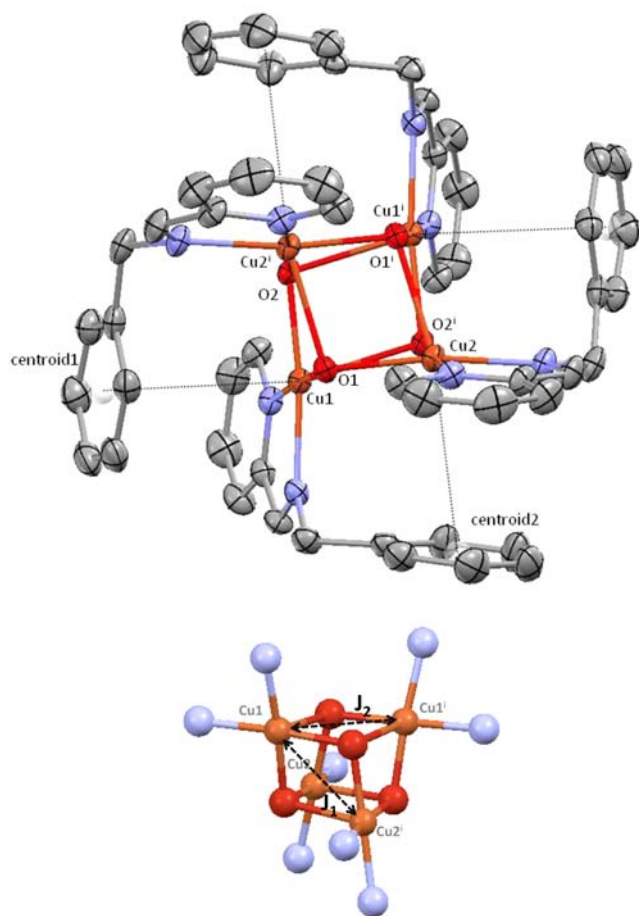


Figure 1. (Top) Thermal ellipsoid plot of **1** showing the atomic displacement parameters at 20% probability (CCDC 915281). Hydrogen atoms, counterions, and the disordered water molecule are omitted for clarity. The cation- π interactions are represented as dashed lines between the copper atoms and the centroids of the aromatic rings ($i: -x, y, 0.5 - z$). (Bottom) Magnetic exchange pathways for the cubane core of **1**.

selected interatomic distances and angles are listed in Table 1. The core of complex **1** is composed of four hydroxo-bridged copper(II) ions symmetrically related by a crystallographic 2-fold

Table 1. Selected Bond Lengths and Angles for Complex 1^a

Interatomic Distances (Å)			
Cu1–N1	2.016(4)	Cu2 ⁱ –O2	1.950(3)
Cu1–N2	2.004(3)	Cu1–O2	1.984(3)
Cu2–N3	1.997(4)	Cu1 ⁱ –O2	2.326(3)
Cu2–N4	2.004(4)	Cu1–O2 ⁱ	2.326(3)
Cu1–O1	1.953(3)	Cu2–O2 ⁱ	1.950(3)
Cu2–O1	1.975(3)	Cu2–O1 ⁱ	2.315(3)
Cu2 ⁱ –O1	2.315(3)		
Angles (deg)			
Cu1–O1–Cu2	103.30(13)	Cu2 ⁱ –O2–Cu1 ⁱ	91.75(11)
Cu1–O1–Cu2 ⁱ	92.39(11)	Cu1–O2–Cu1 ⁱ	101.52(12)
Cu2–O1–Cu2 ⁱ	100.82(13)		
Copper–Centroid Distances (Å)			
Cu1–centroid1	3.598	Cu2–centroid2	3.591

^aSymmetry code: (i) $-x, y, -z + 1/2$.

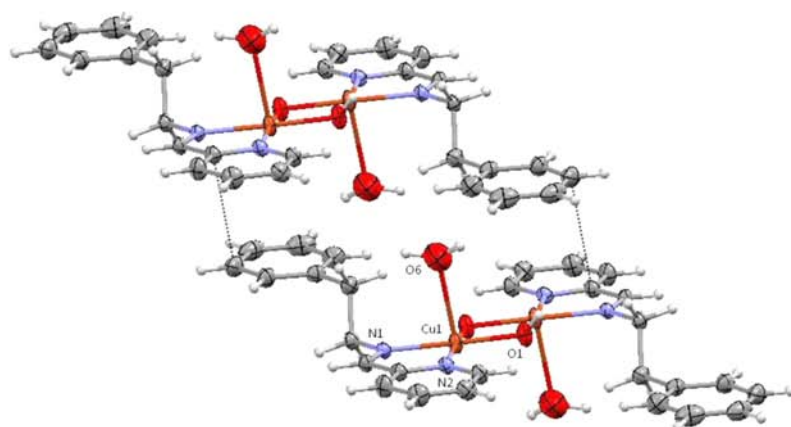
axis, forming a cubane-like structure. Structural indices were calculated as described by Addison et al.²⁴ for five-coordinate structures in order to measure the degree of trigonality ($\tau = 0$ for a perfect square-pyramidal geometry and $\tau = 1$ for a perfect trigonal-bipyramidal geometry). The copper ions are in square-pyramidal geometries, as confirmed by the values of the structural indices: $\tau = 0.053$ for Cu1 and $\tau = 0.093$ for Cu2, indicating small deviations from perfect square-pyramidal geometries. The equatorial coordination positions are occupied by the two nitrogen atoms from the ligand and two oxygen atoms from hydroxide bridges. The Cu–N distances are found to range from 1.997 to 2.016 Å. The Cu–O distances for hydroxides in equatorial or axial positions range from 1.950 to 1.984 Å and from 2.315 to 2.326 Å, respectively. These Cu–O distances are in the range of distances found in other known $\text{Cu}_4(\text{OH})_4$ cubanes (see the Supporting Information, Figure S1).¹³ Finally, analysis of the distances within the cubane core reveals that complex **1** clearly belongs to the $[4 + 2]$ category, with Cu1...Cu2 and Cu1...Cu2ⁱ ($i: -x, y, 0.5 - z$) and their two symmetry-related counterparts being significantly shorter (3.081 and 3.090 Å, respectively) than the Cu1...Cu1ⁱ and Cu2...Cu2ⁱ distances (3.345 and 3.312 Å, respectively).

Interestingly, the phenyl substituents of the ligands are located at apical positions above the copper(II) ions with a distance between the metal ion and centroid of the ring of ca. 3.59 Å indicative of intramolecular metal cation- π interactions. No intermolecular π -type interactions are detected (Supporting Information, Figure S2). Cation- π interactions are increasingly recognized as important noncovalent forces having a stabilizing role in the structure of various molecules including proteins.²⁵ Many examples of metal cation- π interactions have been described, with alkali metals strengthening the importance of such noncovalent forces in the stabilization, the reactivity, and even the selectivity in chemistry and biology. However, this interaction is not yet generally recognized as an important structural motif in the chemistry of copper(II) complexes, although several metal cation- π interactions have been evidenced involving copper(II) ions.²⁶ Finally, to the best of our knowledge, this unusual interaction has never been evidenced in copper(II) cubane structures and appears as an important stabilizing parameter of the tetranuclear core.

In order to study the effect of the length of the chain between the coordinated imine and phenyl ring on the structure of the core, a complex was prepared using ligand **L**². In this case, and using strictly the same experimental procedure, a binuclear hydroxo-bridged complex **2** was obtained. The molecular structure of the cation of complex **2** is presented in Figure 2. Selected bond lengths and angles are listed in Table 2. Complex **2** is composed of two hydroxo-bridged copper(II) ions. The metal ion is in square-pyramidal geometry ($\tau = 0.067$),²⁴ with the basal plane occupied by the nitrogen atoms of **L**² and the hydroxo groups. The Cu–N distances are found to range from 1.993 to 2.004 Å. The Cu–O distances for the bridging hydroxides are found at ca. 1.91 Å. A water molecule is found in the axial position at 2.61 Å from the copper ion. Unlike complex **1**, no intramolecular interaction involving the phenyl ring is observed. The phenyl substituents are rather involved in π - π interactions with the pyridine rings of neighboring binuclear complexes, leading to chainlike structures in the solid state.

Finally, slight modification of the synthetic procedure using **L**² led to formation of the mononuclear complex **3**. The molecular structure of **3** is presented in Figure 2. Selected bond lengths and angles are listed in Table 2. The copper ion is bound to two **L**²

A



B

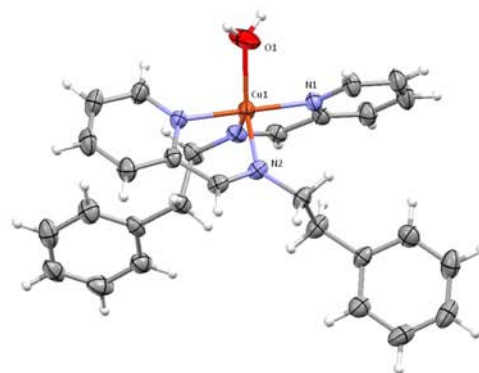


Figure 2. (A) Thermal ellipsoid plot of **2** showing the molecular structure atomic displacement parameters at 30% probability and the packing via intermolecular π - π interactions between the aromatic rings. Counteranions are omitted for clarity. (B) Thermal ellipsoid plot of **3** showing the atomic displacement parameters at 30% probability. Counteranions are omitted for clarity.

Table 2. Selected Bond Lengths and Distances for Complexes 2 and 3^a

complex 2		complex 3	
Interatomic Distances (Å)			
N1–Cu1	1.993(2)	N1–Cu1	1.975(4)
N2–Cu1	2.004(2)	N2–Cu1	2.090(3)
Cu1–O1	1.910(2)	O1–Cu1	2.037(5)
Cu1–O1 ⁱ	1.916(2)	Cu1–N1 ⁱⁱ	1.975(4)
Cu1–O6	2.617(6)	Cu1–N2 ⁱⁱ	2.090(3)
Angles (deg)			
Cu1–O1–Cu1 ⁱ	99.43(9)	N1–Cu1–N1 ⁱⁱ	179.9(2)
O1–Cu1–O1 ⁱ	80.57(9)	N1–Cu1–O1	90.06(10)
O1–Cu1–N1	179.04(9)	N1 ⁱⁱ –Cu1–O1	90.06(10)
O1 ⁱ –Cu1–N1	98.81(9)	N1–Cu1–N2	80.77(14)
O1–Cu1–N2	98.74(9)	N1 ⁱⁱ –Cu1–N2	99.16(14)
O1 ⁱ –Cu1–N2	175.15(10)	O1–Cu1–N2	124.24(9)
N1–Cu1–N2	81.94(9)	N1–Cu1–N2 ⁱⁱ	99.16(14)
O1–Cu1–Cu1 ⁱ	40.36(6)	N1 ⁱⁱ –Cu1–N2 ⁱⁱ	80.77(14)
O1 ⁱ –Cu1–Cu1 ⁱ	40.20(6)	O1–Cu1–N2 ⁱⁱ	124.24(9)
N1–Cu1–Cu1 ⁱ	139.01(7)	N2–Cu1–N2 ⁱⁱ	111.52(18)
N2–Cu1–Cu1 ⁱ	138.90(7)		

^aSymmetry code: (i) $-x + 2, -y + 1, -z + 2$; (ii) $-x + 2, y, -z + 3/2$.

ligands and a water molecule in a distorted trigonal-bipyramidal geometry (structural index $\tau = 0.92$). The structure is similar to that obtained with a different counteranion.¹⁶

Magnetic Properties. The magnetic behavior of complex **2** was measured from 300 to 2 K (Figure 3A). The value of the product (χT) of the molar susceptibility (χ) and the temperature (T) is $0.61 \text{ cm}^3 \text{ K mol}^{-1}$ at room temperature, slightly smaller than $0.75 \text{ cm}^3 \text{ K mol}^{-1}$ expected for two copper(II) ions (assuming $g = 2.0$). As the temperature is lowered, the χT value decreases and χ presents a maximum at 180 K, indicative of an antiferromagnetic interaction between the copper(II) ions. The increase of χ at low temperature reveals the presence of a small amount of paramagnetic impurities. The magnetic properties of complex **2** were described using the following spin Hamiltonian:

$$H = -J(\hat{S}_{\text{Cu1}} \cdot \hat{S}_{\text{Cu1}^i})$$

The susceptibility data can be fitted to the Bleaney–Bowers equation (eq 1), where g is the gyromagnetic ratio, ρ is the

amount of paramagnetic impurities, and TIP is the temperature-independent paramagnetism.²⁷ The paramagnetic impurity is assumed to be a monomer $S = 1/2$ with a molecular weight half that of the dimer.

$$\chi = (1 - \rho) \frac{2N\beta^2 g^2}{kT \left[3 + \exp\left(-\frac{J}{kT}\right) \right]} + \rho\chi_{\text{imp}} + \text{TIP} \quad (1)$$

The best fit was obtained with $J = -221.3 \text{ cm}^{-1}$, $g = 2.12$, and $\rho = 1.7\%$. Magnetostructural correlations for binuclear hydroxo-bridged copper(II) complexes have been established by Hatfield et al.⁵ A linear correlation has been determined between the Cu–O–Cu bond angle (θ) and the exchange coupling constant J . In addition, an antiferromagnetic coupling is predicted for θ larger than 98° , and a ferromagnetic coupling is predicted for smaller angles. In the case of complex **2**, the value of the Cu–O–Cu angle (99.4°) is consistent with the observed antiferromagnetic interaction. Although the Cu–O–Cu angle is a crucial parameter, the coupling constant can be modulated by other structural features. This can explain that the constant obtained from simulation ($J = -221 \text{ cm}^{-1}$) is higher in absolute value than the predicted one ($J = -139 \text{ cm}^{-1}$).

The magnetic behavior of complex **1** was measured from 300 to 2 K. The temperature dependence of χT and χ are displayed in Figure 3B. At room temperature, the product χT is $1.53 \text{ cm}^3 \text{ K mol}^{-1}$, a value consistent with the presence of four $S = 1/2$ copper(II) ions (1.50 assuming $g = 2$). The product χT decreases continuously from room temperature to 2 K, indicating the predominance of antiferromagnetic interactions. The increase of the susceptibility χ at low temperature indicates the presence of a small amount of $S = 1/2$ paramagnetic impurities. The structural properties of complex **1** are in agreement with the $[4 + 2]$ category of cubanes, and because of the presence of a C_2 axis, the magnetic properties of complex **1** should be described by the following spin Hamiltonian:²⁸

$$H = -J_{12}(2\hat{S}_{\text{Cu1}} \cdot \hat{S}_{\text{Cu2}}) - J_{12}^i(2\hat{S}_{\text{Cu1}^i} \cdot \hat{S}_{\text{Cu2}^i}) - J_{11}^i(\hat{S}_{\text{Cu1}} \cdot \hat{S}_{\text{Cu1}^i}) - J_{22}^i(\hat{S}_{\text{Cu2}} \cdot \hat{S}_{\text{Cu2}^i})$$

However, to avoid overparameterization, the coupling scheme was simplified by taking $J_{12} = J_{12}^i = J_1$ and $J_{11}^i = J_{22}^i = J_2$.

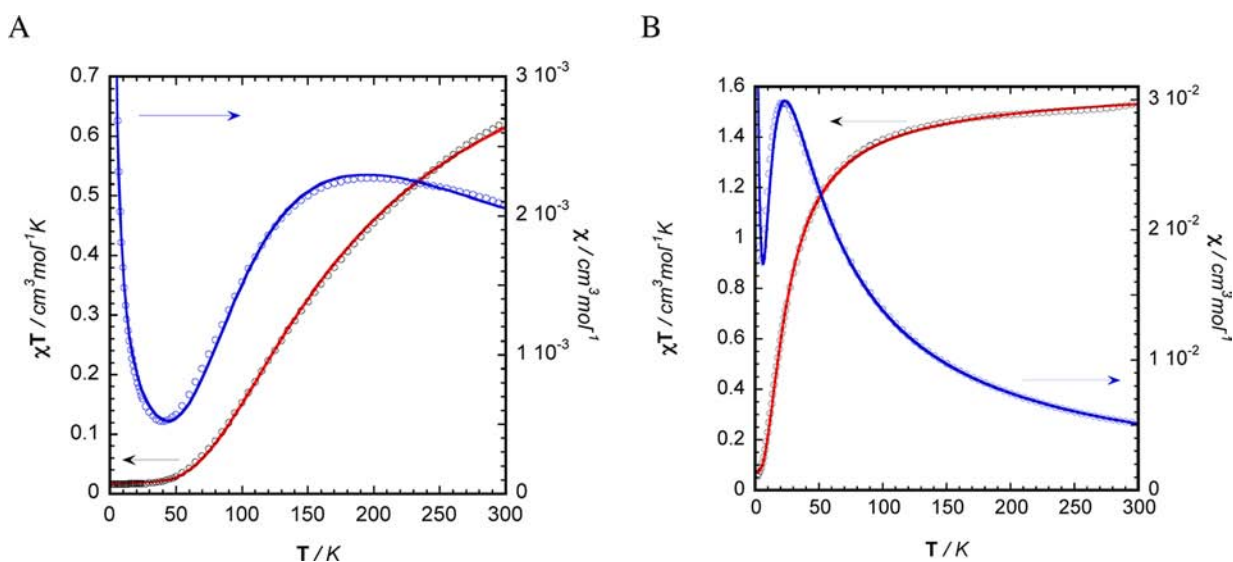


Figure 3. (A) Temperature dependence of χ (O (blue), experimental data; — (blue), best fit) and χT (O (black), experimental data; — (red), best fit) for complex 2: best fit with values $g = 2.12$, $J = -221.3 \text{ cm}^{-1}$, paramagnetic impurity $\rho = 1.7\%$, TIP = $120 \times 10^{-6} \text{ cm}^3 \text{ mol}^{-1}$, $R_\chi = 3.0 \times 10^{-4}$, and $R_{\chi T} = 1.4 \times 10^{-4}$. (B) Temperature dependence of χ (O (blue), experimental data; — (blue), best fit) and χT (O (black), experimental data; — (red), best fit) for 1: best fit with values $g = 2.05$, $J_1 = -21.7 \text{ cm}^{-1}$, $J_2 = 7.6 \text{ cm}^{-1}$, paramagnetic impurity = 6.5%, TIP = $62 \times 10^{-6} \text{ cm}^3 \text{ mol}^{-1}$, $R_\chi = 2.7 \times 10^{-3}$, and $R_{\chi T} = 4.0 \times 10^{-5}$.

The susceptibility was therefore fitted according to the following equation (eq 2), where the parameters g and TIP have the same meaning as those in the previous case and ρ is the amount of monomeric $S = 1/2$ impurity with a molecular weight a quarter of that of the tetramer.

$$\chi_{\text{exp}} = (1 - \rho)\chi_{\text{cubane}} + \rho\chi_{\text{imp}} + \text{TIP} \quad (2)$$

$$\chi_{\text{cubane}} = \frac{2N\beta^2 g^2}{kT} \{ [2 \exp(-y) + \exp(-x) + 5 \exp(x)] / [\exp(-2y) + 6 \exp(-y) + \exp(-2x) + 3 \exp(-x) + 5 \exp(x)] \}$$

$$\text{with } x = \frac{J_1}{kT} \quad \text{and} \quad y = \frac{J_2}{kT}$$

The fit procedure leads to $J_1 = -21.7 \text{ cm}^{-1}$ and $J_2 = 7.6 \text{ cm}^{-1}$ with $g = 2.05$ and $\rho = 6.5\%$. In the case of $[4 + 2]$ cubanes, the presence of long Cu–O bond distances in the exchange pathways complicates the estimation of the coupling constant values by strictly applying magnetostructural correlations used for symmetric hydroxo-bridged dinuclear complexes.⁷ In our case, the J_2 coupling constant corresponds to exchange pathways exhibiting two short and two long Cu–O distances (~ 1.98 and $\sim 2.32 \text{ \AA}$, respectively). Thanks to theoretical calculations, Tercero et al. have shown that, in the case of two short and two long distances, a ferromagnetic interaction that is little dependent on the Cu–O–Cu angle is obtained.⁷ This is in good agreement with our positive value of $J_2 = 7.6 \text{ cm}^{-1}$ even though Cu–O–Cu angles are greater than 98° . The J_1 coupling constant corresponds to the four exchange pathways with three short ($\sim 1.96 \text{ \AA}$) and one long ($\sim 2.32 \text{ \AA}$) Cu–O distances. According to the work of Tercero et al., the sign of the coupling should be correlated, with the exchange pathway displaying the shortest Cu–O distances. In the case of complex 1, the pathway displaying the shortest Cu–O distances is associated with a Cu–O–Cu angle of ca. 103.5° and an antiferromagnetic coupling is therefore expected. In addition, the coupling is also

expected to be weaker than that in the case of symmetric dimers. This is therefore consistent with the rather small determined antiferromagnetic coupling constant $J_1 = -21.7 \text{ cm}^{-1}$.

Evaluation of the Energy of Metal– π Interaction. There are only a few data on the energy of copper(II)– π interactions, and calculations were performed to confirm the presence of a metal– π interaction in complex 1 and to quantify this interaction. The use of a dispersion-corrected DFT has been shown to be crucial for a similar copper(II)– π interaction.²⁹ On the basis of the work of Chakravorty et al., who have compared different functionals to describe similar interactions,³⁰ we performed calculations using the *wB97XD* functional that includes empirical dispersion.²⁰ We first considered the model system (Figure 4A) formed by the phenyl group, one copper ion, three

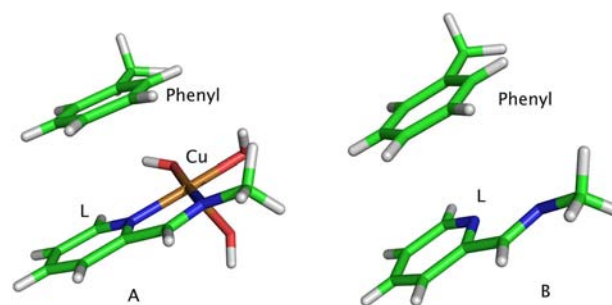


Figure 4. Systems considered for the DFT calculations in order to estimate the contributions of π -type interactions in the cubane complex. The positions of the atoms are fixed to their respective position in the crystal structure of 1: (A) phenyl ring lies above a part of L^1 with Cu(OH)₃; (B) phenyl ring lies above a part of L^1 without copper.

hydroxo groups, and the part of the ligand L^1 that is bound to the metal. The different groups were set exactly at their positions in the X-ray structure of complex 1. The interaction energy between the phenyl group and the rest of the system (ligand + hydroxo groups + copper), called Ph and S, respectively, is defined by eq 3.

$$E_{\text{int}} = E_{\text{S-Ph}}^{\text{C}} - E_{\text{S}}^{\text{C}} - E_{\text{Ph}}^{\text{C}} \quad (3)$$

where E_{S-ph}^C is the electronic energy of the whole system and E_{Ph}^C and E_S^C are the energies of each of the components, the phenyl ring and the rest of the system, isolated and set at positions equal to those in the whole system, based on X-ray data. A value of 9 kcal mol⁻¹ is obtained for the interaction energy. It corresponds to the stabilization effect due to the metal- π interaction but also to the π - π interaction suggested by the partial alignment of the two aromatic groups. To estimate the contribution of this π - π interaction, a similar calculation was then performed on a similar model system without the copper ion (Figure 4B). The interaction energy was computed to 4 kcal mol⁻¹.

The difference between the interaction energies of the full system with copper and the system without copper is 5 kcal mol⁻¹ and corresponds to the metal cation- π interaction. This value is comparable to the energy of copper(II)- π interactions calculated in other systems.^{26,29} Therefore, for the complete system (cubane with four copper ions), it is possible to give an evaluation of stabilization of the cubane thanks to the metal- π interactions of 20 kcal mol⁻¹.

CONCLUSION

In conclusion, playing with the length of the aliphatic chain between the imine and phenyl ring allowed us to tune between intra- and intermolecular π -type interactions involving the aromatic substituents of the ligands. In the case of complex **1**, whereas no intermolecular interactions are present, the intramolecular copper- π interactions appear as major stabilization parameters for the cubane core, accounting for ca. 20 kcal mol⁻¹ of the total energy of the complex. Therefore, this interaction probably acts as a driving parameter for the aggregation process. With more flexibility (complex **2**), no intramolecular π -type interactions are detected but rather intermolecular π - π interactions stabilizing a binuclear complex.

ASSOCIATED CONTENT

Supporting Information

X-ray crystallographic data for **1**–**3** in CIF format. Distribution of Cu–O distances in cubane complexes. Packing diagram of **1**. This material is available free of charge via the Internet at <http://pubs.acs.org>.

AUTHOR INFORMATION

Corresponding Author

*E-mail: jalila.simaan@univ-amu.fr. Tel: +33 491289151.

Notes

The authors declare no competing financial interest.

ACKNOWLEDGMENTS

The authors gratefully acknowledge Prof. Jean-Jacques Girerd for useful advice and discussion. This work was financially supported by the Provence-Alpes Côte d'Azur (PACA) region (Grant DEB10-924 2010-12144).

REFERENCES

- (1) Aromí, G.; Brechin, E. K. *Struct. Bonding (Berlin)* **2006**, *122*, 1–68.
- (2) Mallah, T.; Marvilliers, A. *Magnetism: Molecules to Materials II*; Wiley-VCH Verlag GmbH & Co.: Weinheim, Germany, 2001; pp 189–226.
- (3) Gatteschi, D.; Sessoli, R. *J. Magn. Magn. Mater.* **2004**, *1030*, 272–276.
- (4) Holm, R. H.; Kennepohl, P.; Solomon, E. I. *Chem. Rev.* **1996**, *96*, 2239–2314.
- (5) Crawford, V. H.; Richardson, H. W.; Wasson, J. R.; Hodgson, D. J.; Hatfield, W. E. *Inorg. Chem.* **1976**, *15*, 2107–2110.
- (6) Ruiz, E.; Alemany, P.; Alvarez, S.; Cano, J. *J. Am. Chem. Soc.* **1997**, *119*, 1297–1303.
- (7) Tercero, J.; Ruiz, E.; Alvarez, S.; Rodriguez-Fortea, A.; Alemany, P. *J. Mater. Chem.* **2006**, *16*, 2729–2735.
- (8) Mergehenn, R.; Merz, L.; Haase, W. *Acta Crystallogr.* **1976**, *B32*, 505–510.
- (9) Haase, W. *J. Mol. Catal.* **1984**, *23*, 331–340.
- (10) Mergehenn, R.; Merz, L.; Haase, W. *J. Chem. Soc., Dalton Trans.* **1980**, 1703–1709.
- (11) Ruiz, E.; Rodriguez-Fortea, A.; Alemany, P.; Alvarez, S. *Polyhedron* **2001**, *20*, 1323–1327.
- (12) Merz, L.; Haase, W. *J. Chem. Soc., Dalton Trans.* **1980**, 875–879.
- (13) Allen, F. H. *Acta Crystallogr.* **2002**, *B58*, 380.
- (14) (a) Dedert, P. L.; Sorrell, T.; Marks, T. J.; Ibers, J. A. *Inorg. Chem.* **1982**, *21*, 3506–3517. (b) Lopez, N.; Vos, T. E.; Arif, A. M.; Shum, W. W.; Noveron, J. C.; Miller, J. S. *Inorg. Chem.* **2006**, *45*, 4325–4327. (c) Ackermann, J.; Meyer, F.; Pritzkow, H. Z. *Anorg. Allg. Chem.* **2004**, *630*, 2627–2631. (d) Kohn, R. D.; Pan, Z.; Mahon, M. F.; Kociok-Kohn, G. *Dalton Trans.* **2003**, 2269–2275. (e) Putzien, S.; Wirth, S.; Roedel, J. N.; Lorenz, I.-P. *Polyhedron* **2011**, *30*, 1747–1751. (f) Sletten, J.; Sorensen, A.; Julve, M.; Journaux, Y. *Inorg. Chem.* **1990**, *29*, 5054–5058. (g) Eberhardt, J. K.; Glaser, T.; Hoffmann, R.-D.; Frohlich, R.; Wurthwein, E.-U. *Eur. J. Inorg. Chem.* **2005**, 1175–1181. (h) Xu, L.; Kim, Y.; Kim, S.-J.; Kim, H. J.; Kim, C. *Inorg. Chem. Commun.* **2007**, *10*, 586–589. (i) Fielden, J.; Sprott, J.; Long, D.-L.; Kogerler, P.; Cronin, L. *Inorg. Chem.* **2006**, *45*, 2886–2895. (j) Jones, L. F.; Kilner, C. A.; Halcrow, M. A. *Polyhedron* **2007**, *26*, 1977–1983. (k) Bowmaker, G. A.; Nicola, C. D.; Marchetti, F.; Pettinari, C.; Skelton, B. W.; Somers, N.; White, A. H. *Inorg. Chim. Acta* **2011**, *375*, 31–40. (l) Lopez, S.; Keller, S. W. *Supramol. Chem.* **1998**, *9*, 239–244.
- (15) Song, Y.; Xu, Z.; Sun, Q.; Su, B.; Gao, Q.; Liu, H.; Zhao, J. *J. Coord. Chem.* **2007**, *60*, 2351–2359.
- (16) Johnson, D. W.; Mayer, H. K.; Minard, J. P.; Banaticla, J.; Miller, C. *Inorg. Chim. Acta* **1988**, *144*, 167–171.
- (17) Otwinowski, Z.; Minor, W. *Macromolecular Crystallography. In Methods in Enzymology*; Carter, C. W., Jr., Sweet, R. M., Eds.; Academic Press: New York, 1997; Vol. 276, Part A, pp 307–326.
- (18) Altomare, A.; Cascarano, G.; Giacovazzo, G.; Guagliardi, A.; Burla, M. C.; Polidori, G.; Camalli, M. *J. Appl. Crystallogr.* **1994**, *27*, 435–436.
- (19) Sheldrick, G. M. *Acta Crystallogr.* **2008**, *A64*, 112–122.
- (20) Chai, J. D.; Head-Gordon, M. *Phys. Chem. Chem. Phys.* **2008**, *10*, 6615–6620.
- (21) Frisch, M. J.; Trucks, G. W.; Schlegel, H. B.; Scuseria, G. E.; Robb, M. A.; Cheeseman, J. R.; Scalmani, G.; Barone, V.; Mennucci, B.; Petersson, G. A.; Nakatsuji, H.; Caricato, M.; Li, X.; Hratchian, H. P.; Izmaylov, A. F.; Bloino, J.; Zheng, G.; Sonnenberg, J. L.; Hada, M.; Ehara, M.; Toyota, K.; Fukuda, R.; Hasegawa, J.; Ishida, M.; Nakajima, T.; Honda, Y.; Kitao, O.; Nakai, H.; Vreven, T.; Montgomery, J. A., Jr.; Peralta, J. E.; Ogliaro, F.; Bearpark, M.; Heyd, J. J.; Brothers, E.; Kudin, K. N.; Staroverov, V. N.; Kobayashi, R.; Normand, J.; Raghavachari, K.; Rendell, A.; Burant, J. C.; Iyengar, S. S.; Tomasi, J.; Cossi, M.; Rega, N.; Millam, J. M.; Klene, M.; Knox, J. E.; Cross, J. B.; Bakken, V.; Adamo, C.; Jaramillo, J.; Gomperts, R.; Stratmann, R. E.; Yazyev, O.; Austin, A.; Cammi, J. R.; Pomelli, C.; Ochterski, J. W.; Martin, R. L.; Morokuma, K.; Zakrzewski, V. G.; Voth, G. A.; Salvador, P.; Dannenberg, J. J.; Dapprich, S.; Daniels, A. D.; Farkas, Ö.; Foresman, J. B.; Ortiz, J. V.; Cioslowski, J.; Fox, D. J. *Gaussian 09*, revision A.1; Gaussian, Inc.: Wallingford, CT, 2009.
- (22) Schaefer, A.; Horn, H.; Ahlrichs, R. *J. Chem. Phys.* **1992**, *97*, 2571–2577.
- (23) (a) Boys, S. F.; Bernardi, F. *Mol. Phys.* **1970**, *19*, 553–566. (b) Simon, S.; Duran, M.; Dannenberg, J. J. *J. Chem. Phys.* **1996**, *105*, 11024–11031.
- (24) Addison, A. W.; Rao, T. N.; Reedijk, J.; van Rijn, J.; Verschoor, G. C. *J. Chem. Soc., Dalton Trans.* **1984**, 1349–1356.

- (25) Salonen, L. M.; Ellerman, M.; Diederich, F. *Angew. Chem., Int. Ed.* **2011**, *50*, 4808–4842.
- (26) (a) Yorita, H.; Otomo, K.; Hiramatsu, H.; Toyama, A.; Miura, T.; Takeuchi, H. *J. Am. Chem. Soc.* **2008**, *130*, 15266–15267. (b) Costa-Filho, A. J.; Nascimento, O. R.; Ghivelder, L.; Calvo, R. *J. Phys. Chem. B* **2001**, *105*, 5039–5047. (c) Heine, K. B.; Clegg, J. K.; Heine, A.; Gloe, K.; Gloe, K.; Henle, T.; Bernhard, G.; Cai, Z.-L.; Reimers, J. R.; Lindoy, L. F.; Lach, J.; Kersting, B. *Inorg. Chem.* **2011**, *50*, 1498–1505. (d) Ishihara, K.; Fushimi, M.; Akakura, M. *Acc. Chem. Res.* **2007**, *40*, 1049–1055.
- (27) Kahn, O. *Molecular Magnetism*; VCH Publishers: New York, 1993.
- (28) Hall, J. W.; Estes, E. W.; Estes, E. D.; Scaringe, P. R.; Hatfield, W. E. *Inorg. Chem.* **1977**, *16*, 1575–1574.
- (29) Helios, K.; Wysokinski, R.; Zierkiewicz, W.; Proniewicz, L. M.; Michalska, D. *J. Phys. Chem. B* **2009**, *113*, 8158–8169.
- (30) Chakravorty, D. K.; Wang, B.; Ucisik, M. N.; Merz, K. M., Jr. *J. Am. Chem. Soc.* **2011**, *133*, 19330–19333.